01 Oct 1993

Two-Dimensional Simulation of Switch-On Speeds in Hydrogenated Amorphous Silicon Thin-Film Transistors

J. S. Huang

Cheng-Hsiao Wu

Missouri University of Science and Technology, chw@mst.edu

Two-dimensional simulation of switch-on speeds in hydrogenated amorphous silicon thin-film transistors

J. S. Huang and C. H. Wu
Department of Electrical Engineering, University of Missouri-Rolla, Rolla, Missouri 65401

(Received 1 March 1993; accepted for publication 25 June 1993)

We report accurate two-dimensional simulations of switch-on speeds in hydrogenated amorphous silicon thin-film transistors. The trap charge density along, or transverse to, the direction of semiconductor channel is highly nonuniform and the trap filling time dominates the switching time as compared to the transit time, which is about four orders of magnitude smaller. Near both contacts, direction of the transverse current is always upwards toward the insulator-semiconductor interface due to the strong electric fields. However, at the central region of the channel, the transient current is quite complex and is discussed here. When the channel length varies from 2 to 10 μm, the switching-on time is of the order of 10^{-3} s. The occupation function everywhere displays a partial filling of higher-energy trap states during the switch-on. This is in contrast to results presented by other investigators. Finally, the relationship between the transit time and the switch-on time with respect to the amount of trap states is discussed.

I. INTRODUCTION

The use of hydrogenated amorphous silicon thin-film transistors (*a*-Si:H TFT) for driving large-area active-matrix liquid-crystal displays has become a commercial reality in recent years. Most of the theoretical investigations[1–6] have been centered on the static characteristics. Notably, Hack[6,7] and Shur[3,8] and their collaborators have investigated various realistic inverted-gate device geometries and contacts with immense success. By comparison, dynamical characteristics have not been as thoroughly studied. The use of disordered materials, such as hydrogenated amorphous silicon, for switching devices presents an interesting and challenging problem to calculate the switching speeds because such calculation is outside the framework of traditional transit-time theory used for crystalline devices. Earlier, Yue *et al.*[9] asserted that the slow switching-on time was due to the large amount of trap charges present in the channel. The result is a much weakened electric field in the mid section of the channel. This fact, coupled with the smaller conduction-band mobility (13 $cm^2/V\,s$), results in a much longer transit time, the time required for the formation of conduction channel. The failure of this model lies in the fact that occupation dynamics of the trap states is not properly evaluated. They have assumed that as soon as electron density changes due to the applied voltage, the quasi-Fermi distribution of the trap states is instantaneously reached. Therefore, the switch-on time is determined by the time-dependent continuity equation for electrons as in the crystalline case. Powell[10,11] has proposed a two-fluid model from the fact that both initial and final trap occupation functions are Fermi-distribution-like and the transition from the initial state to the final state is exponential in time with a characteristic switching time $\tau(\epsilon)$ as a function of the trap state energy ϵ. This model misjudged the nature of trapping dynamics as we will discuss later in this work. Bullock and one of the authors[12] were the first to evaluate complete dynamics of trap filling and trap emptying in one-dimensional geometry. In particular, a partial filling of higher-energy trap states during the switch-on is clearly shown. In this work, we present the first accurate results of two-dimensional simulation of switch-on times. The finite thickness of the semiconductor channel is such that there are large differences of both free-carrier and trap charge densities at the semiconductor-insulator interface and at the semiconductor-substrate interface. The switch-on time is then determined by the nonuniform filling of trap states in the entire semiconductor channel. In particular, there is an increased upward movement of free-carrier towards the semiconductor-insulator interface at the later part of the switch-on. In Sec. II we discuss the physical model and the appropriate two time-dependent equations involved for free-carrier density and the occupation function of trap states for our simulations. The reason that trap-filling dynamics dominate the switch-on time is clearly demonstrated. The numerical method used is briefly described in Sec. III. Four cases of numerical computations are presented here and discussed in Sec. IV. Section V contains our conclusions.

II. PHYSICAL MODEL OF *a*-Si:H TFT

The device under investigation is an insulated-gate field-effect transistor (IGFET). The model is restricted to a single-gate device, although a similar model could be developed for a double-gate IGFET.[1] A simple device geometry is shown in Fig. 1. The semiconductor layer consists of *a*-Si:H that is generally intrinsic or mildly *n* type with doping concentration N_D and the source and drain consist of a heavily doped *n*-type *a*-Si:H. Experimentally, it has been observed that contacts of nearly all metals with *a*-Si:H are low resistance or ohmic,[13] so the source and drain interfaces with the semiconductor are essentially ohmic.

The geometric parameters specified in the device model are the channel length L, the semiconductor layer thickness t_s, and the insulator thickness t_i. The material

 0021-8979/93/74(8)/5231/10/$6.00

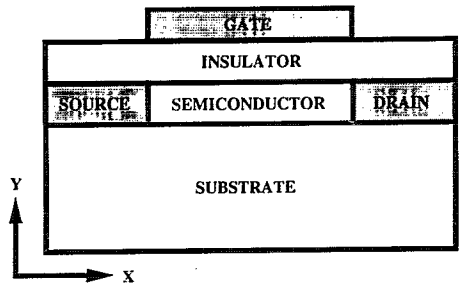

FIG. 1. Device geometry of *a*-Si:H TFTs.

parameters are the semiconductor doping concentration N_D, of the channel between the source and the drain, the insulator and semiconductor dielectric permittivity, ϵ_i and ϵ_s, and the semiconductors diffusivity D_n. The source contact (at $x=0$) is taken to be at ground potential. When no voltage is applied to the gate, the energy bands are assumed to be flat. When a positive-gate voltage is applied, negative charges are pulled from the source and the drain and accumulated near the insulator-semiconductor interface to form a conducting channel. In our two-dimensional computational model, current flows between the source and drain contacts (i.e., x direction) and between the semiconductor-substrate and insulator-semiconductor interfaces (i.e., y direction).

The two-dimensional Poisson equation can be written as

$$\frac{\partial^2\varphi}{\partial x^2}+\frac{\partial^2\varphi}{\partial y^2}=-\frac{\rho}{\epsilon_s}, \tag{1}$$

where the space charge ρ is the sum of free electron n, ionized dopant N_D^+, and trap charges from donorlike states $N_D(\epsilon)$ and acceptorlike states $N_A(\epsilon)$, so that

$$\rho=q\left(-n+N_D^+ + \int N_D(\epsilon)[1-f(\epsilon)]d\epsilon - \int N_A(\epsilon)f(\epsilon)d\epsilon\right), \tag{2}$$

where $f(\epsilon,x,y,t)$ is the occupation function, which is a function of trap state energy ϵ, position (x,y), and time t and will be discussed later. The donorlike states can be approximated from experimental results as

$$N_D(\epsilon)=\left(\frac{N_v}{kT}\right)e^{(\epsilon_v-\epsilon)/\epsilon_D} \tag{3}$$

and similarly

$$N_A(\epsilon)=\left(\frac{N_c}{kT}\right)e^{(\epsilon-\epsilon_c)/\epsilon_A}, \tag{4}$$

where $\epsilon_D=43$ meV and $\epsilon_A=27$ meV are used.[14]

Using the dimensionless unit of potential $V=q\varphi/kT$, the 2D Poisson equation can be written as

$$\frac{\partial^2 V}{\partial x^2}+\frac{\partial^2 V}{\partial y^2}=\frac{q^2}{kT\epsilon_s}\left(N_c e^{V-E}-N_D^+ - \int [N_D(1-f)-N_A f]d\eta\right), \tag{5}$$

where the free-electron density $n=N_c e^{V-E}$, E is the dimensionless quasi-Fermi level, and $\eta=q\epsilon/kT$ is the dimensionless energy.

The dynamics of the occupation function for trap states f can be appropriately described by a rate equation based on Simmons and Taylor's theory for continuous distributions of trap states.[15] The occupation of a particular trap level is controlled by two opposing processes of capture into the trap and emission into the conduction band. Thus,

$$\frac{df}{dt}=\sigma v n(1-f)-e_n f, \tag{6}$$

where σ is the capture cross section, v is the thermal velocity, and e_n is the emission rate that is determined by the equilibrium condition so that

$$e_n=\sigma v N_c e^{\eta}. \tag{7}$$

Thus, Eq. (6) is simplified to

$$\frac{df}{dt}=\sigma v N_c e^{V-E}[1-f(1+e^{\eta-V+E})]. \tag{8}$$

If we consider *a*-Si:H as a unipolar device so that generation and recombination effects can be neglected, then the time-dependent 2D continuity equation can be written as

$$\frac{\partial\rho}{\partial t}+\frac{\partial J_{nx}}{\partial x}+\frac{\partial J_{ny}}{\partial y}=0, \tag{9}$$

where the first term of Eq. (9) contains the displacement current through the Poisson equation. The conduction current and the electron current are identical, which in the x direction is J_{nx}, and in the y direction is J_{ny}. J_{nx} and J_{ny} are given by

$$J_{nx}=-qD_n n\frac{\partial E}{\partial x}, \qquad J_{ny}=-qD_n n\frac{\partial E}{\partial y}. \tag{10}$$

As we have shown here, there are two time derivatives, df/dt of Eq. (8) and $\partial\rho/\partial t$ of Eq. (9). In the examples shown later, we prove that the switching speed is dominated by the df/dt term and not by the $\partial\rho/\partial t$ term. This is the essence of disproving the transit-time theory. The time derivative of space charge ρ in Eq. (9) can be obtained from Eq. (2) to yield the current continuity equation that is expressed in terms of variable E, the quasi-Fermi level, and can be written as

$$\frac{\partial^2 E}{\partial x^2}+\frac{\partial E}{\partial x}\left(\frac{\partial V}{\partial x}-\frac{\partial E}{\partial x}\right)+\frac{\partial^2 E}{\partial y^2}+\frac{\partial E}{\partial y}\left(\frac{\partial V}{\partial y}-\frac{\partial E}{\partial y}\right)$$
$$=-\frac{1}{Dn}\left(\frac{\partial V}{\partial t}-\frac{\partial E}{\partial t}+\sigma v\int (N_D+N_A)\right.$$
$$\left.\times[1-f(1+e^{\eta-V+E})d\eta]\right). \tag{11}$$

The drain current per unit length is determined by

$$I_D=-\int_0^{t_s} J_{nx}(x=L)dy \tag{12}$$

and the source current per unit length is given by

$$I_S=-\int_0^{t_s} J_{nx}(x=0)dy. \tag{13}$$

The gate current per unit length is caused by the displacement current only and is determined as

$$I_G=-\int_0^{t_s}\int_0^{L}\frac{\partial \rho}{\partial t}dx\,dy=I_S-I_D. \tag{14}$$

In our model, there are no trap charges inside the insulator, and the substrate layer is floating so that the electric field inside is zero. The boundary conditions at the semiconductor-substrate interface ($y=0$), and the insulator-semiconductor interface ($y=t_s$) for the Poisson equation can be determined by the continuity of dielectric displacement at both interfaces. The interface charges are neglected. Thus

$$\frac{\partial V}{\partial y}(y=t_s)=\frac{\epsilon_i}{\epsilon_s}\frac{(V_G-V)}{t_i} \tag{15}$$

and

$$\frac{\partial V}{\partial y}(y=0)=0. \tag{16}$$

Now consider the boundary conditions at these interfaces for the continuity equation, since $J_{ny}=0$ at both interfaces. The boundary conditions to solve Eq. (11) are

$$\frac{\partial E}{\partial y}(y=t_s)=0 \tag{17}$$

and

$$\frac{\partial E}{\partial y}(y=0)=0. \tag{18}$$

III. NUMERICAL METHOD

We note that the inclusion of a dynamical equation for trap occupation in Eq. (8) makes all numerical programs available for crystalline devices invalid for our calculations. In our formulation the three differential equations (2D Poisson equation, 2D continuity equation, and occupation equation of trap states) are coupled to each other. We have developed a new numerical scheme to solve simultaneously two coupled second-order 2D differential equations [Eqs. (5) and (11), and a third first-order nonlinear differential equation Eq. (8)]. The two partial differential equations

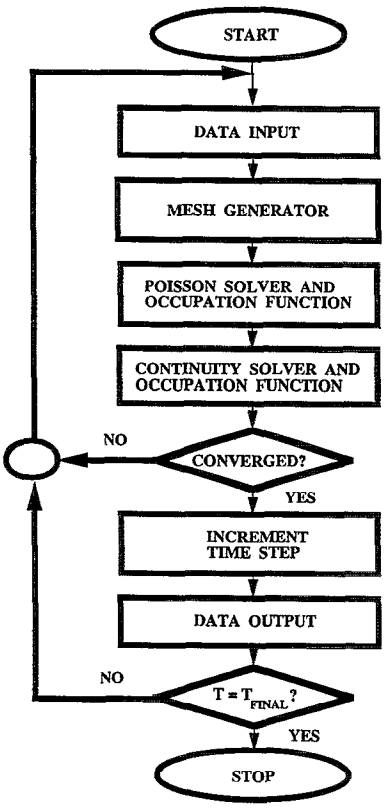

FIG. 2. Flow chart of the program.

and the first-order differential equation are of the following form for variables V, E, and f, as a function of position (x,y), and time t

$$\frac{\partial^2 V}{\partial x^2}+\frac{\partial^2 V}{\partial y^2}=g_1(V,E,f),$$

$$\frac{\partial^2 E}{\partial x^2}+\frac{\partial E}{\partial x}\left(\frac{\partial V}{\partial x}-\frac{\partial E}{\partial x}\right)+\frac{\partial^2 E}{\partial y^2}+\frac{\partial E}{\partial y}\left(\frac{\partial V}{\partial y}-\frac{\partial E}{\partial y}\right)=g_2(V,E,f), \tag{19}$$

$$\frac{df}{dt}=g_3(V,E,f).$$

Our two-dimensional results have been obtained using implicit finite-difference techniques. A nonuniform mesh and newly developed higher-accuracy finite difference equations were used to obtain an accurate solution. The first-order equation is solved by a single-step backward Euler method. The system of equations set up by the finite-difference equations is solved using a Newton–Raphson method. The method described above has been implemented in a computer program as shown by the flow charts illustrated in Fig. 2. An adaptive nonuniform mesh of 400×30 is used along the semiconductor channel and an equally spaced mesh of 100 points in the energy gap is used to adequately represent the continuous energy distribution of the occupation function. The occupation function $f(\epsilon,x,y,t)$ thus requires a fairly large storage memory. The iterative computings during the drastic change of carrier

density that occurs at $10^{-7} \leqslant t \leqslant 10^{-4}$ s require a typical computing time of 100 h at each time step using an IBM RISC/6000 model 550 computer.

IV. RESULTS AND DISCUSSIONS

Equations (5), (8), and (11) are solved for V, f, and E at every point (x,y) in the semiconductor layer for a given time t using the following input parameters:

$D_n = 0.33$ cm^2/s, $T = 300$ K,

$N_D = 10^{12}$ cm^{-3}, $t_s = 10^{-5}$ cm,

$t_i = 10^{-5}$ cm, $\epsilon_s = 11.0$, and $\epsilon_i = 3.9$.

In the first example, we show a case in which both the gate and drain-source voltages are turned on simultaneously from the equilibrium condition. At turn-on voltages of $\varphi_{DS} = 5$ V, $\varphi_G = 10$ V, and the channel length $L = 10$ μm, the free-electron concentration is shown in Fig. 3 for successive intervals of time. At $t = 10^{-14}$ s [Fig. 3(a)], the concentration is almost uniform as in the case of equilibrium. At that interval, the Poisson equation resembles the Laplace equation, because no appreciable space charge has flowed into the layer. At $t = 10^{-9}$ s, the two peaks of Fig. 3(b) near the source and the drain indicate that extra electrons are being drawn into the layer from the source and drain contact. At $t = 10^{-6}$ s [Fig. 3(c)], which is the order of the transit time, the channel is only weakly formed. This is still far from the steady state. At $t = 10^{-5}$ s [Fig. 3(d)], a roughly smooth layer exists except near the source and drain contacts. The pulled-in charges are accumulated mainly on the immediate region of the insulator-semiconductor interface. There is a two- to three-times difference in the magnitude of the free-carrier density in the y direction. The free-carrier density is still two orders of magnitude below the steady-state value, which is reasonably reached at $t > 10^{-4}$ s [Fig. 3(e)]. The free charges increase everywhere until $t \cong 10^{-5}$ s. From $t \cong 10^{-5}$ s on, the region further away from the insulator-semiconductor interface begins to reach the steady-state value, but the free charges keep increasing near the interface region. This is achieved by an increased upward movement of free carriers toward the interface near the source and drain regions. At the steady-state condition [Fig. 3(f)], there is a difference of about 50 times of magnitude in the free-carrier density in the y direction that is exhibited. In the switch-on of a-Si:H TFTs, the free-carrier concentration will increase only in cooperation with the filling of the trap states. This can be observed from the filling of the corresponding acceptorlike states as shown in Figs. 4(a)–4(c). Note the similarity in the shape of each figure as compared to the corresponding free-carrier density figures [Figs. 3(b), 3(c), and 3(f)], except that the order of magnitude is about one higher. Also note that the peak positions in the x direction in Fig. 4(a) are a little closer to the source and drain contacts than in Fig. 3(b). We note that capturing time for the trap states is proportional to the inverse of the capture rate, and is of the order of 10^{-8} s. Thus, when $t \leqslant 10^{-8}$ s, the acceptorlike-charge density shows a little "delay" compared to the free-charge density.

The occupation function, $f(\epsilon,x,y,t)$, depends on gap state energy, as well as position, (x,y), in the semiconductors' layer. At $x = 0.5L$ and $y = t_s$, $f(\epsilon,t)$ is shown in Fig. 5 at various time intervals. At time $t = 10^{-14}$ s [curve (a)], f is almost an equilibrium Fermi distribution. At steady state [curve (d)], the Fermi level ϵ_f is shifted about 0.35 eV toward the conduction band. However, at any intermediate state a non-Fermi distribution is obtained. It is evident that at $t = 10^{-6}$ s [curve (b)], the quasi-equilibrium approximation, or the two-fluid model, fails to obtain the correct result and consequently, the correct switch-on time. If curve (b) is approximated by a Fermi distribution with a time-dependent ϵ_f, the net effect is that higher-energy trap states are filled "completely" too quickly. Curve (b) clearly indicates "partially" filled higher-energy trap states. Thus, the quasi-equilibrium approximation grossly underestimates the time to reach steady state as in the work by Matsumura *et al.*[9] The trap occupation dynamics have also been analyzed by Van Berkel *et al.*[11] However, their calculations are based on an inaccurate two-fluid model for the occupation function, which can be written as

$$f(\epsilon,t) = [\, f(\epsilon,\epsilon_{f_0}) - f(\epsilon,\epsilon_f)\,]\, e^{-t/\tau(\epsilon)} + f(\epsilon,\epsilon_f),$$

where $f(\epsilon,\epsilon_{f_0})$ and $f(\epsilon,\epsilon_f)$ are the initial and final Fermi distributions. This equation implies that the transient occupation is expressible in terms of fractions of initial and final Fermi distributions. Clearly, it is impossible to obtain the results of curve (b) and curve (c) in Fig. 5 from their model distribution function because the partial filling is not uniform over the range between ϵ_{f_0} and ϵ_f. In crystalline FETs, the time-dependent continuity equation (or dn/dt term) determines the switch-on time, which is on the order of the transit time because of the drift-diffusion mechanism described in the transport equation. However, the dynamic behavior of the a-Si:H TFTs in the switch-on situation is determined by two distinct processes; the first is the transport of free carriers from the source and drain contacts (dn/dt term), and the second is the trapping into and the emission from the deep localized states (df/dt term). These two processes, or the two time derivatives, dominate at different time scales. From Fig. 3 we show that the switch-on time is at least the order of 10^{-4} s. Thus, the switch-on time of a-Si:H TFTs is determined by the capture process of electrons described by $df/dt \approx \sigma v n(1-f)$, which is much larger than the dn/dt term in the continuity equation. Therefore, the switch-on time is the time required to fill all the trap states from the equilibrium ϵ_{f_0} level up to the steady-state ϵ_f level, and is not the transit time. The $f(\epsilon,t)$ at $x = 0.5L$ and $y = 0.5t_s$ is shown in Fig. 6. From $t = 10^{-14}$ s to $t = 10^{-6}$ s [curves (a) and (b)], f is about the same as in Fig. 5. From $t = 10^{-5}$ s to steady state [curves (c) and (d)], it indicates that the amount of higher-energy trap states filled at $y = 0.5t_s$ is less than that at the insulator-semiconductor interface. By comparing Fig. 5 with Fig. 6, we observe that the accumulation of trap

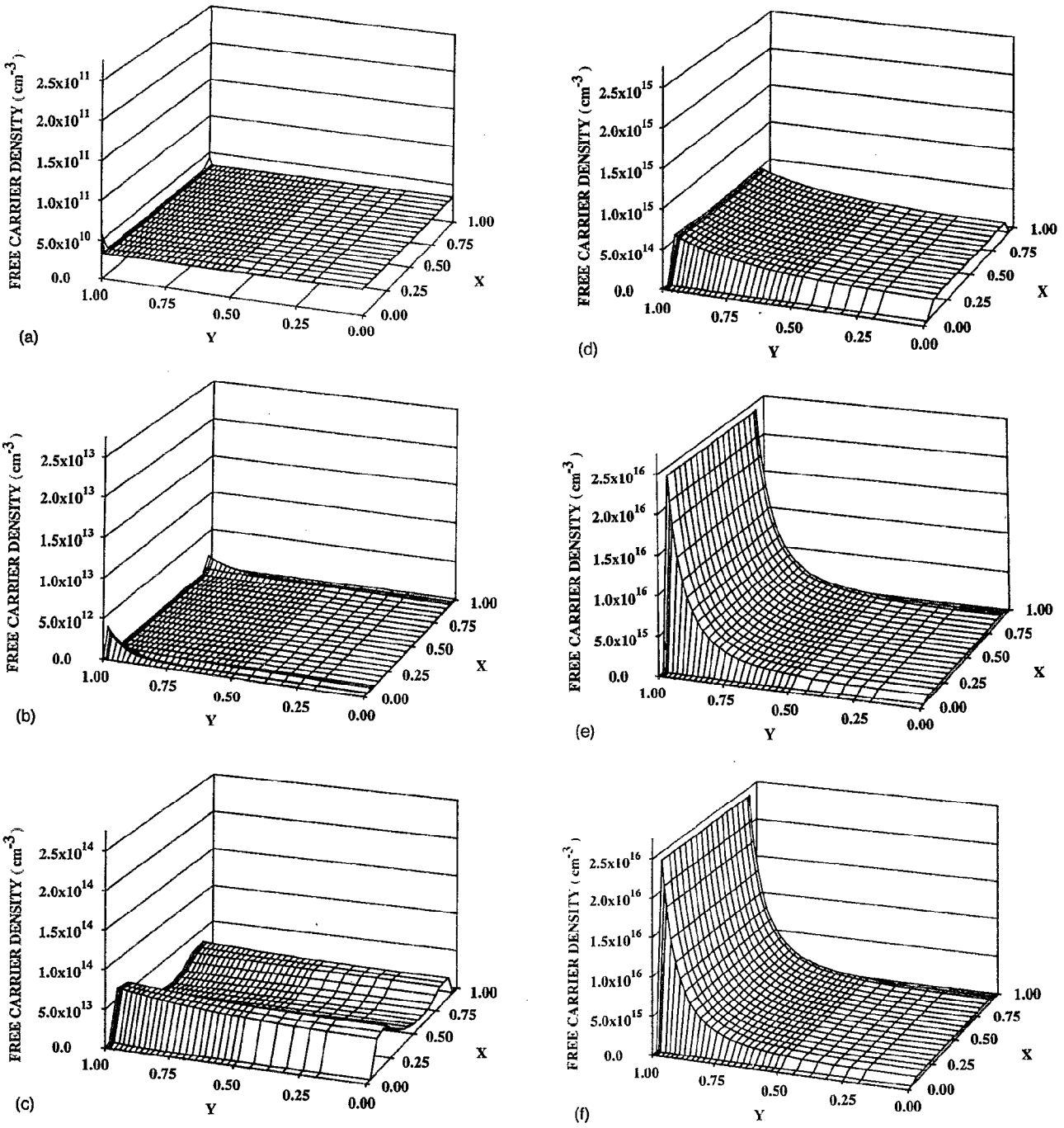

FIG. 3. Free-carrier density for $\varphi_{DS}=5$ V, $\varphi_G=10$ V, and $L=10$ μm. Each figure is for a different time: (a) 10^{-14} s, (b) 10^{-9} s, (c) 10^{-6} s, (d) 10^{-5} s, (e) 10^{-4} s, (f) steady state.

charges is in cooperation with the free-carrier concentration, with a time lag of trap-capturing time.

The switch-on time can be evaluated clearly through the terminal currents (I_G, I_S, and I_D), which are shown in Fig. 7. Initially, electrons are pulled from the source and drain contacts into the channel, thus I_S is positive and I_D is negative. Since the free-carrier density increases with time, I_G is positive and equals I_S-I_D. When electrons are finally pulled from the source contact into the channel and then flow into the drain contact from the channel, both I_S and I_D are positive. The free-carrier density approaches steady state and I_G approaches zero. At $t\cong 10^{-3}$ s, terminal currents are more or less steady and this time can be considered as the switch-on time. Note that this is three to four orders of magnitude greater than the transit time. It has been reported that the steady state drain current is a function of the doping concentration.[16,17] DeWever[16] has shown that when N_D increases by two orders, the magnitude of the steady state I_D also increases two orders. Therefore, our value of current density (A/cm in Fig. 7) is in

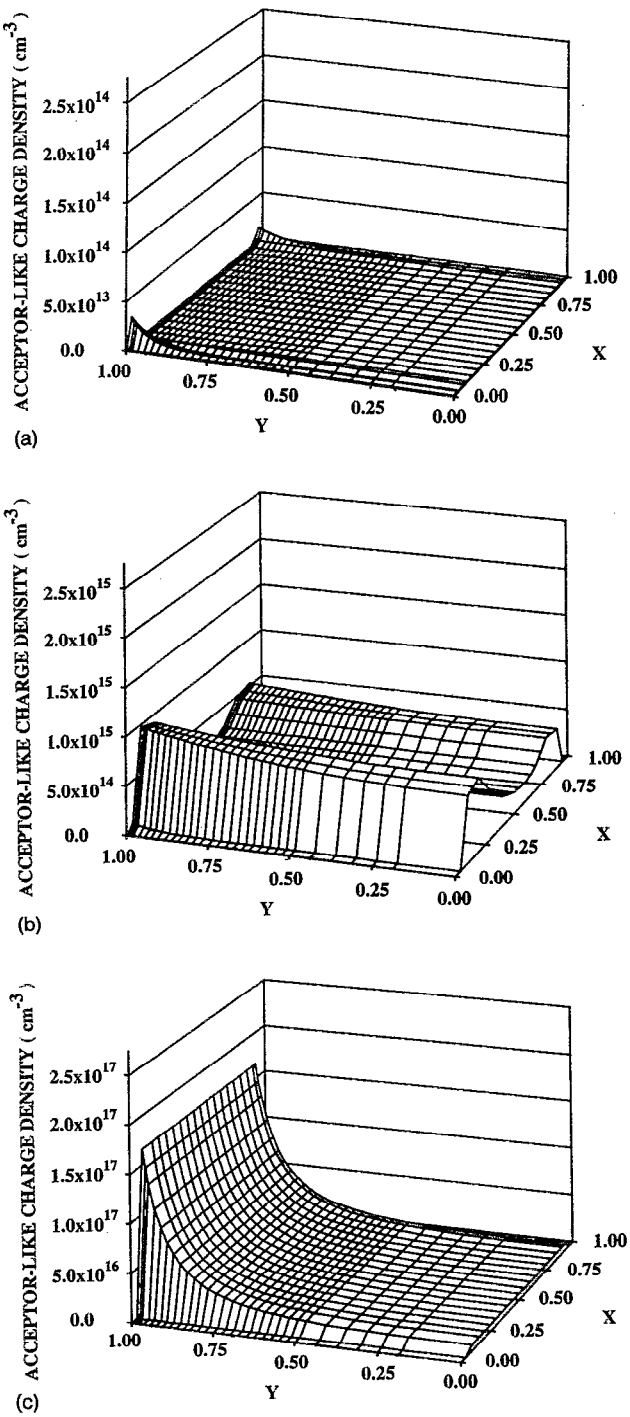

FIG. 4. Charged acceptorlike state density for $\varphi_{DS}=5$ V, $\varphi_G=10$ V, and $L=10$ μm. Each figure is for a different time: (a) 10^{-9} s, (b) 10^{-6} s, (c) steady state. Note the similarity in the density profile of each figure as compared to the corresponding free-electron figure in Fig. 3, except that the order of magnitude is about one higher. Also note that the peak positions in the x direction in (a) are slightly closer to the source and drain contacts than in Fig. 3(b).

good agreement with the experimental results in Ref. 17.

In the second example, we show a situation similar to the first example with a reduced channel length. At turn-on voltages of $\varphi_{DS}=2.5$ V, $\varphi_G=5$ V, and the channel length $L=2$ μm, the transit time will be shown in Fig. 8 to be about 10^{-8} s, which is two orders of magnitude less than

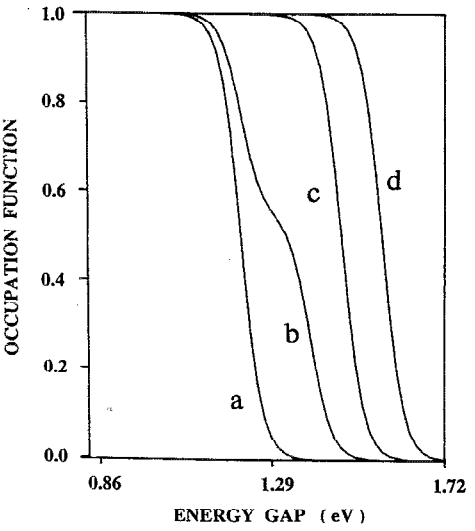

FIG. 5. Occupation function at $x=0.5L$, $y=t_s$, for $\varphi_{DS}=5$ V, $\varphi_G=10$ V, and $L=10$ μm. Each curve is for a different time: (a) 10^{-14} s, (b) 10^{-6} s, (c) 10^{-5} s, (d) 10^{-4} s to steady state. Energy of 1.72 eV is located at the mobility edge of the conduction band. Note the partially filled higher-energy trap dstates in curve (b).

the transit time of the first case. Note that the transit time formula given by $t=L^2/\mu\varphi_{DS}$ is not valid for estimating transit time in amorphous silicon transistors. This expression is accurate only if the electric potential along the channel is fairly linear. In a-Si:H TFTs, the electric potential in the channel varies extremely nonlinear. Near the source and drain contacts the electric field is very high, but the weak electric field in the midsection of the channel causes the transit time to be much longer. In our example, the electric field in the source or drain regions is roughly

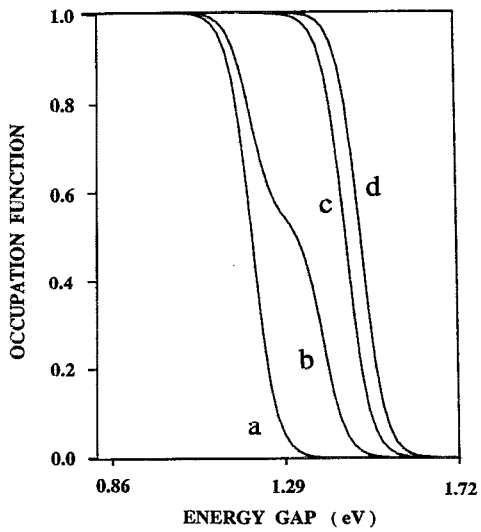

FIG. 6. Occupation function at $x=0.5L$, $y=0.5t_s$, for $\varphi_{DS}=5$ V, $\varphi_G=10$ V, and $L=10$ μm. Each curve is for a different time: (a) 10^{-14} s, (b) 10^{-6} s, (c) 10^{-5} s, (d) 10^{-4} s to steady state. Comparing to Fig. 5, it is shown that when the location is further away from the insulator-semiconductor interface, the steady-state Fermi-level shift, $\epsilon_f - \epsilon_{f_0}$, is smaller.

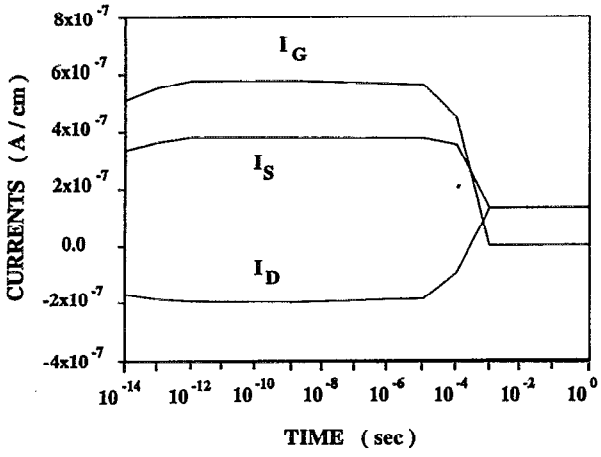

FIG. 7. Terminal currents I_D, I_S, and I_G per unit channel width vs time for $\varphi_{DS}=5$ V, $\varphi_G=10$ V, and $L=10$ μm. Switch-on time of about 10^{-3} s is clearly shown.

five to six orders of magnitude higher than that in the midsection of the channel. Thus, the time when the two free-carrier density peaks merge together to form a weekly conducting channel [for example, Fig. 8(a)] is much longer than one traditionally estimates using the formula with linear-potential approximation. The free-carrier concentration in the channel is shown in Fig. 8. At $t=10^{-14}$ s, the free-carrier concentration is essentially at the equilibrium value. However, at $t=10^{-8}$ s [Fig. 8(a)], which is the order of the transit time, the channel is only weakly formed. The two peaks in the figure show that electrons are pulled in from both the source and the drain contacts. Again, this is far from the steady state. As we indicated in the first example, a large number of electrons are required to fill the trap states in order to provide the channel with enough free electrons. At $t=10^{-5}$ s [Fig. 8(b)], a smooth conducting layer exists except near the source and drain contacts. At $t=10^{-4}$ s [Fig. 8(c)], near steady state is reached. Again, the pulled-in charges are accumulated on the immediate region of the insulator-semiconductor interface. The free-carrier concentration at steady state, in the y direction, shows a more than two orders of magnitude difference. By comparing Fig. 8 with Fig. 3, it is clear that when the channel is longer, the flat, or smooth, region of the free-carrier concentration is extended and the transit time is much larger. The filling of acceptorlike trap states follows a trend similar to the buildup of free electrons except that the amount is one order of magnitude higher, as shown in Fig. 9. The occupation functions at $x=0.5L$ and $y=t_s$ are shown in Fig. 10 for various time intervals. In Fig. 10, curves (b) and (c) show a drastic change of occupation function from $t=10^{-7}$ s to $t=10^{-6}$ s. This clearly shows how acceptorlike states are filled "gradually" in a manner totally different from the Fermi distribution or the two-fluid model. At $t=10^{-4}$ s, the ϵ_f reaches its steady state value [curve (e)]. The terminal currents I_G, I_S, and I_D are shown in Fig. 11. The switch-on time is also approximately at $t=10^{-3}$ s. This is five orders of magnitude greater than the transit time. We note that, in the second

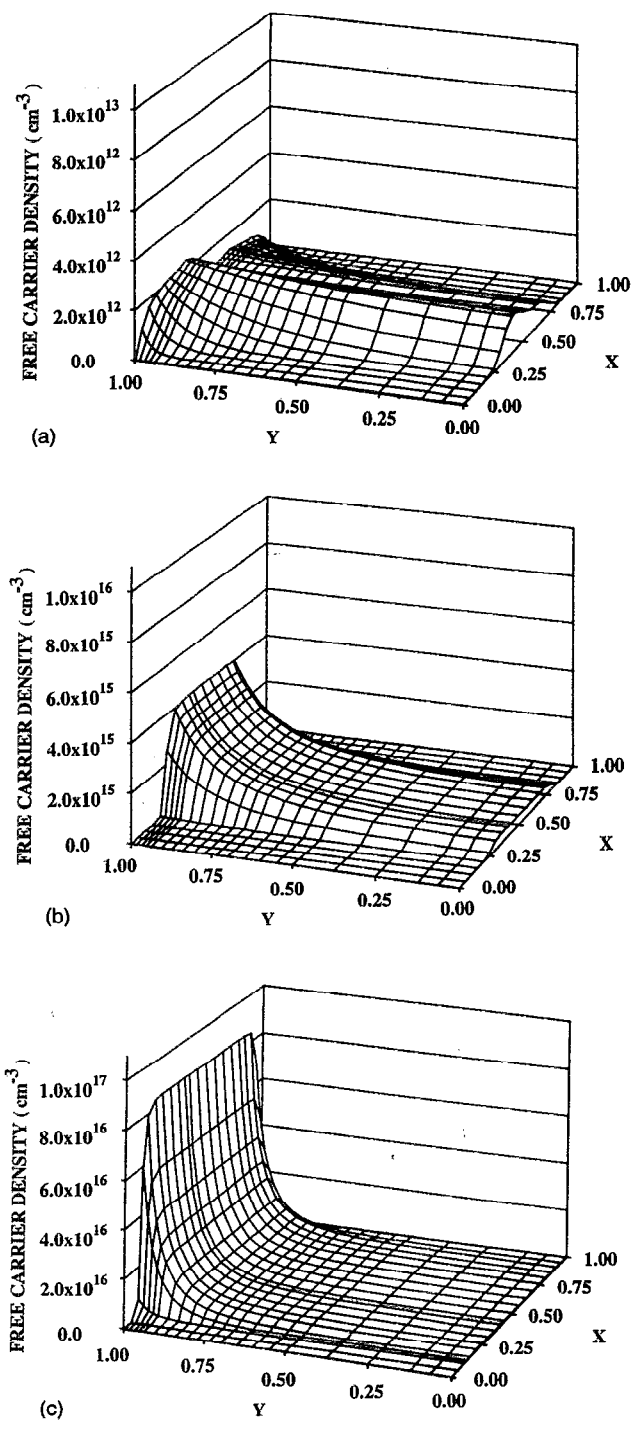

FIG. 8. Free-carrier density for $\varphi_{DS}=2.5$ V, $\varphi_G=5$ V, and $L=2$ μm. Each figure is for a different time: (a) 10^{-8} s, (b) 10^{-5} s, (c) 10^{-4} s to steady state. Here, 10^{-8} s is the transit time as compared to 10^{-6} s in Fig. 3(c).

case, the transit time is about two orders of magnitude less than that in the first case. However, the switch-on time is the same order for both cases. Thus, the switch-on time is determined by the df/dt term, since $df/dt \approx \sigma v n(1-f)$ is about the same for both cases. If the dn/dt term is to be competitive with the df/dt term, the transit time has to be about 10^{-3} s, which requires that the channel length L be about 1 cm in the second case. The transient behavior of

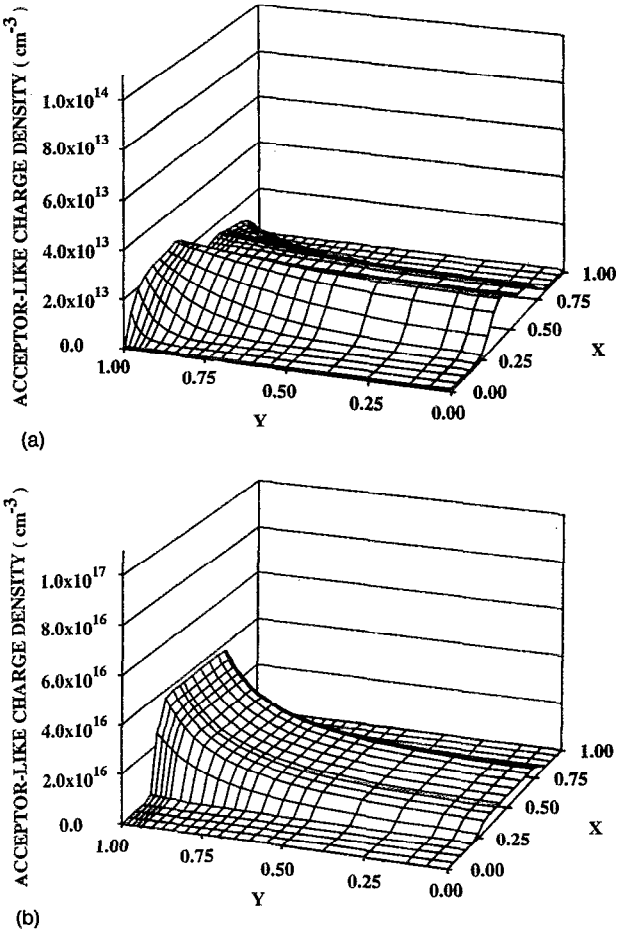

FIG. 9. Charged acceptorlike state density for $\varphi_{DS}=2.5$ V, $\varphi_G=5$ V, and $L=2$ μm. Each figure is for a different time: (a) 10^{-8} s, (b) 10^{-5} s.

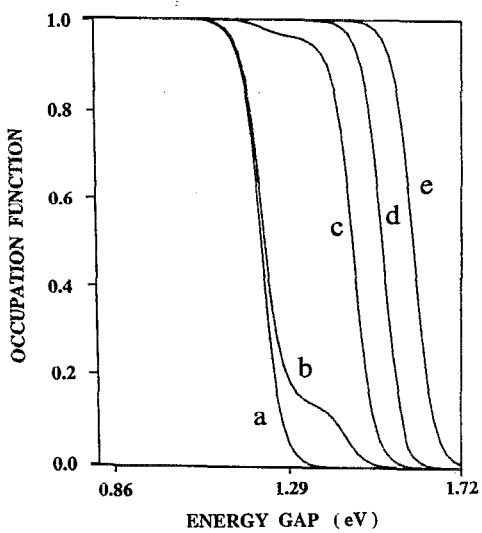

FIG. 10. Occupation function at $x=0.5L$, $y=t_s$ for $\varphi_{DS}=2.5$ V, $\varphi_G=5$ V, and $L=2$ μm. Each curve is for a different time: (a) 10^{-14} s, (b) 10^{-7} s, (c) 10^{-6} s, (d) 10^{-5} s, (e) 10^{-4} s to steady state. This shows that a reduced channel length does not change the relation between free-carrier density and charged acceptorlike state density. Note the partially filled higher-energy trap states at 10^{-7} and 10^{-6} s.

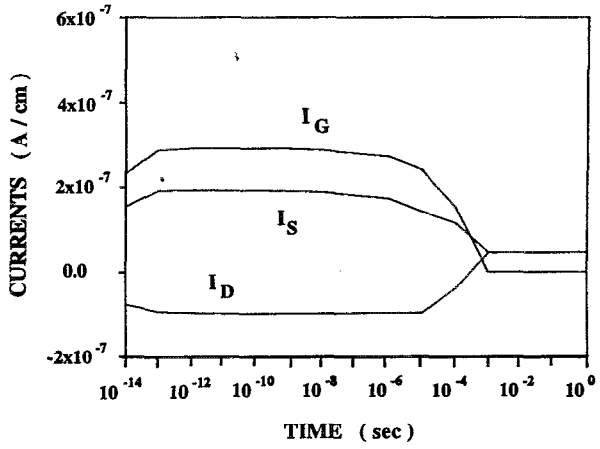

FIG. 11. Terminal currents I_D, I_S, and I_G per unit channel width vs time for $\varphi_{DS}=2.5$ V, $\varphi_G=5$ V, and $L=2$ μm. Note the switch-on time is the same order as in Fig. 7 with a shortened channel.

the electron current in the x direction (J_{nx}) and in the y direction (J_{ny}) is quite complex. At $t=10^{-14}$ s, the electric field is the strongest near the source and drain contacts in both the x and y directions. At this interval, the free-carrier density is almost the same as the equilibrium value. Thus, the total electron currents are contributed entirely by the drift currents. Thus, electrons are pulled in from both contacts and immediately pushed up into the insulator-semiconductor interface by the strong electric field. The magnitudes of J_{nx} and J_{ny} are about the same at this time. At $t=10^{-10}$ s, J_{nx} current reflects a picture that electrons are still pulled in from both contacts and are pushed up into the insulator-semiconductor interface. However, the J_{nx} is now about one order of magnitude higher than the J_{ny} at the same position. From $t=10^{-10}$ s to $t=10^{-4}$ s, J_{nx} is one to two orders of magnitude higher than J_{ny}. At $t=10^{-8}$ s, the transit time, J_{nx} current, indicates that electrons are still pulled into the channel from both contacts. But the J_{ny} current behaves quite differently. Since the electric field is very weak in both directions at the central region of the channel, the diffusion current becomes competitive with the drift current. In the y direction, electrons are pushed up into the insulator-semiconductor interface near both contacts. But, at the central region of the channel, electrons are pushed down from the insulator-semiconductor interface to the semiconductor-substrate interface. The number of pushed-up electrons is about one order of magnitude higher than the pushed-down electrons. This behavior continues until $t=10^{-4}$ s. At $t=10^{-4}$ s, the peak locations where electrons are pushed into the insulator-semiconductor interface shifted to the region away from the contacts and closer to the central region of the channel. This is why the free-electron density has a significant change at $t\cong 10^{-4}$ s. From $t=10^{-4}$ s to steady state, electrons are pulled in from the source contact to the channel, and flow through the channel into the drain contact. Thus J_{nx} reaches a steady state value, and J_{ny} approaches zero everywhere eventually. The increase of free-carrier density as shown in Figs. 8(a) through 8(c) reflects

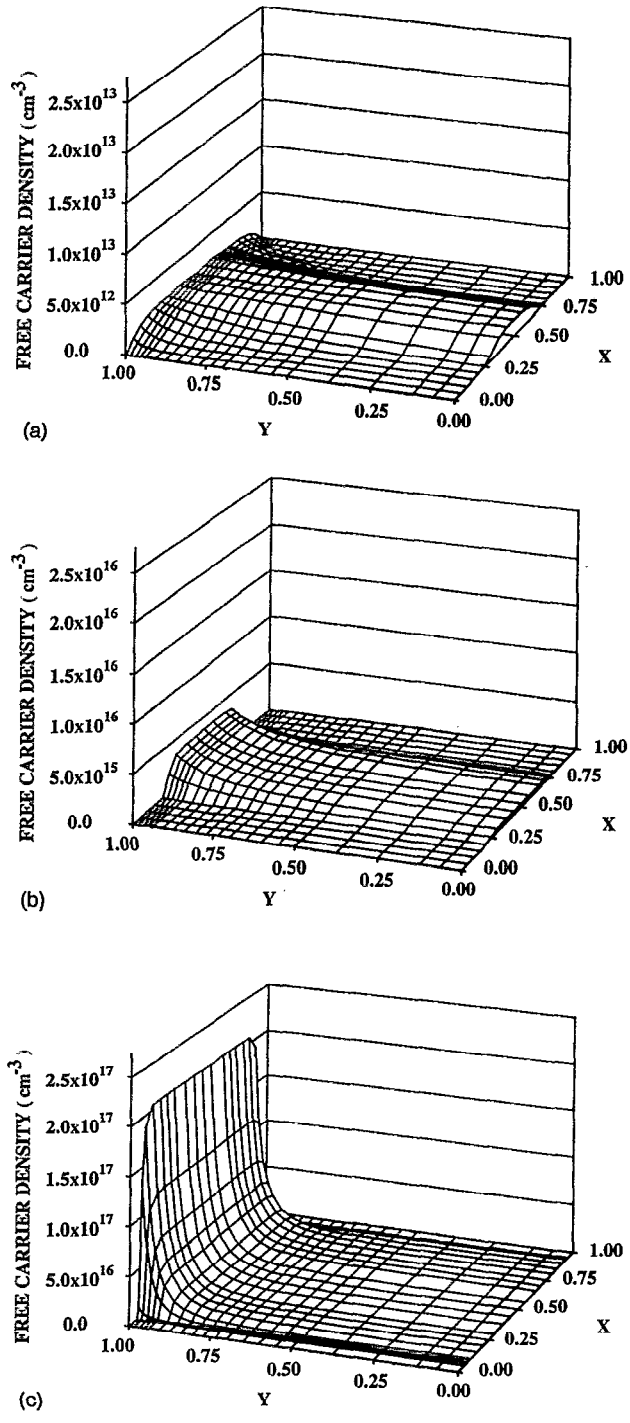

FIG. 12. Free-carrier density for $\varphi_{DS}=0.25$ V, $\varphi_G=5$ V, and $L=2$ μm. Each figure is for a different time: (a) 10^{-8} s, (b) 10^{-5} s, (c) 10^{-4} s to steady state. Comparing to Fig. 8, the peak positions are more symmetric and magnitude of the density is higher.

the behavior of J_{nx} and J_{ny} as discussed above.

In the third example, we show a case that is the same as the second example, except the drain source voltage is reduced to 0.25 from 2.5 V. The free-carrier concentration is shown in Fig. 12. Comparing Fig. 12 with Fig. 8, it indicates that when φ_{DS} is decreased from 2.5 to 0.25 V, the amount of total pull-in charges increases two times at any given time, and the spatial distribution of the free-

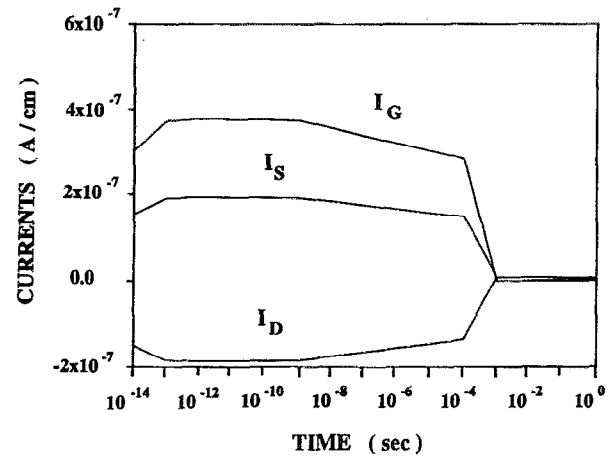

FIG. 13. Terminal currents I_D, I_S, and I_G per unit channel width vs time for $\varphi_{DS}=0.25$ V, $\varphi_G=5$ V, and $L=2$ μm. Comparing to the second case, despite there is higher free-carrier density, the switch-on time remains $\sim 10^{-3}$ s.

carrier density is more symmetrical in the third case than in the second case. Note that the small φ_{DS} implies a more or less pure capacitance effect. The terminal currents are shown in Fig. 13. Again, the switch-on time is about 10^{-3} s.

Finally, we discuss our fourth numerical computation. The donorlike states and acceptorlike states are the same in the previous three examples. To further prove that the switch-on time constant is determined by the capture process of electrons, and not by the transit time, we compute a case that is the same as the third example except that the amount of acceptorlike states is reduced by about 23% with $\epsilon_A=20.7$ meV (Ref. 8) instead of 27 meV. The results verify our expectation. In this situation, the free-carrier density is about one order of magnitude higher than that in the third example and the trap charge density is only four times higher than the free-carrier density instead of one order magnitude higher as in the case of the third example. The net result is that both transit time and switch-on time are reduced approximately by 23% as compared to the third example, and the magnitude of the terminal current is increased by a factor of 5. If the trap state density is reduced continuously to zero, then the switch-on time is shortened continuously to become identical with the transit time.

V. CONCLUSIONS

We present the first accurate system of 2D equations and numerical results for the dynamical characteristics of *a*-Si:H TFTs. We show that the time required to fill the trap states from the equilibrium ϵ_{f_0} up to the steady state ϵ_f determines the switch-on time constant, which is three to five orders of magnitude greater than the transit time. During the switch-on, the occupation function is non-Fermi distributionlike and non-two-fluid- model-like, and exhibits a nonuniform partial filling of higher-energy trap states at any position inside the channel. This is the dynamical picture that others have failed to accurately pro-

vide. Charges are continuously pulled in from both the source and the drain contacts before the steady state is reached and those charges are accumulated mainly at the immediate region of the insulator-semiconductor interface to exhibit a two order of magnitude difference in the transverse direction of the channel at the steady state condition. During the switch-on, the free and trap charges increase everywhere at first, and from $t \cong 10^{-5}$ s on, the region further away from the insulator-semiconductor interface begins to reach the steady state value first. Thus, the charges will have to keep increasing faster near the insulator-semiconductor interface region. This is achieved by a complex two-dimensional movement of charges toward the interface as discussed.

Finally, we show that if the amount of trap states is reduced by 23%, both the transit time and the switch-on time are shortened linearly with respect to the trap-state reduction. This trend continuously approaches to a limiting case when the switch-on time becomes the transit time if the amount of trap states is reduced to zero.

ACKNOWLEDGMENTS

We acknowledge and thank J. N. Bullock for his computer programming assistance during the early stages of this investigation. We are also very grateful to Joy Kung for her help with numerous and crucial numerical works throughout the course of this simulation.

[1] I. Chen and F. C. Luo, J. Appl. Phys. **52**, 3020 (1981).
[2] I. Chen, J. Appl. Phys. **56**, 396 (1984).
[3] M. S. Shur, M. Hack, and C. Hyun, J. Appl. Phys. **56**, 382 (1984).
[4] W. Lee, G. W. Neudeck, J. Choi, and S. Luan, IEEE Trans. Electron Devices **ED-38**, 2070 (1991).
[5] M. J. Powell and J. Pritchard, J. Appl. Phys. **54**, 3244 (1983).
[6] J. G. Shaw and M. Hack, J. Appl. Phys. **65**, 2124 (1989).
[7] M. Hack and J. Shaw, J. Appl. Phys. **68**, 5337 (1990).
[8] M. Shur, M. Hack, and J. Shaw, J. Appl. Phys. **66**, 3371 (1989).
[9] J. Yue, S. Oda, and M. Matsumura, Jpn. J. Appl. Phys. **27**, L919 (1988).
[10] C. van Berkel, J. R. Hughes, and M. J. Powell, Mater. Res. Soc. Symp. Proc. **95**, 445 (1987).
[11] C. van Berkel, J. R. Hughes, and M. J. Powell, J. Appl. Phys. **66**, 4488 (1989).
[12] J. N. Bullock and C. H. Wu, J. Appl. Phys. **69**, 1041 (1991).
[13] M. H. Cohen, H. Fritzsche, and S. R. Ovshinsky, Phys. Rev. Lett. **22**, 1065 (1969).
[14] T. Tiedje, J. M. Celbulka, D. L. Morel, and B. Abeles, Phys. Rev. Lett. **46**, 1425 (1981).
[15] J. G. Simmons and G. W. Taylor, Phys. Rev. B **4**, 1541 (1971).
[16] M. L. DeWever, thesis, University of Missouri-Rolla, 1989.
[17] W. J. Sah, J. L. Lin, and S. C. Lee, IEEE Trans. Electron Devices **ED-38**, 676 (1991).